NORTHWESTERN MEDICAL JOURNAL

Northwestern Med J. 2026;6(2):122-130
DOI: 10.54307/NWMJ.2026.227

RESEARCH ARTICLES

The impact of intervertebral morphological structure on the cobb angle in patients with adolescent idiopathic scoliosis

Mahmut Kurtboğan[1], **Cemal Alkan**[1], **Cengiz Işık**[1], **Metin Çelik**[2], **Emre Arıkan**[3], **Mahmut Timur Turhan**[1], **Mehmet Murat Bala**[4]

[1]Department of Orthopedics and Traumatology, Bolu Abant Izzet Baysal University Medical School, Bolu, Türkiye
[2]Department of Orthopedics and Traumatology, Malatya Training and Research Hospital, Malatya, Türkiye
[3]Bursa Ali Osman Sönmez Oncology Hospital, Bursa, Türkiye
[4]Department of Orthopedics and Traumatology, Aksaray Training and Research Hospital, Aksaray, Türkiye

Cite as: Kurtboğan M, Alkan C, Işık C, et al. The impact of intervertebral morphological structure on the cobb angle in patients with adolescent idiopathic scoliosis. Northwestern Med J. 2026;6(2):122-130.

ABSTRACT

Objective: We aimed to investigate how the heights of the vertebral bodies on the concave and convex sides, as well as the differences between these heights, affect the Cobb angle in patients presenting with adolescent idiopathic scoliosis (AIS).

Materials and Methods: Radiographs and computed tomography (CT) images of 23 patients aged 13-18 years diagnosed with AIS were retrospectively analyzed. The heights of the vertebral bodies on the concave and convex sides were measured and compared with the curvatures determined using the Cobb method. The contributions of the vertebral body Cobb angle and the intervertebral disc Cobb angle to the total Cobb angle were also evaluated.

Results: The vertebral body Cobb angle contributed an average of 52% to the total Cobb angle, while the intervertebral disc Cobb angle contributed an average of 48%. A stronger correlation was observed between the intervertebral disc Cobb angle and the total angle than between the vertebral body Cobb angle and the total angle.

Conclusion: The reduced heights of both the intervertebral disc and the vertebral body on the concave side compared to the convex side indicate that as the difference between these values decreases, these components progressively move away from the apical vertebrae. This causes greater wedging at the apex and reduced wedging in adjacent segments, consequently increasing the total Cobb angle. Although the vertebral body Cobb angle contributes more numerically to the total Cobb angle, the relationship between the intervertebral disc Cobb angle and the total Cobb angle was found to be statistically stronger.

Keywords: scoliosis surgery, young adult idiopathic scoliosis, scoliosis, cobb angle, adolescent idiopathic scoliosis

Corresponding author: Mahmut Kurtboğan **E-mail:** kurtbogann@gmail.com
Received: 27.10.2025 **Accepted:** 28.11.2025 **Published:** 10.04.2026

INTRODUCTION

Defined as a lateral spinal curvature of 10 degrees or more in the frontal plane on standing plain radiographs, scoliosis is the most common spinal deformity; it is a three-dimensional deformity comprising frontal, sagittal, and axial planes. In anomalies causing a lateral shift in the frontal plane, axial rotation and extension in the sagittal plane can be observed, which leads to lordosis (1). Adolescent idiopathic scoliosis (AIS) is observed in approximately 2-4% of healthy children on average and accounts for approximately 80% of structural scoliosis cases occurring at any age during the growth period. AIS can be diagnosed by excluding neurological causes, relevant pathologic findings (e.g., skin lesions in neurofibromatosis), and congenital anomalies through thorough physical and radiological examinations (1).

Although factors such as genetics, growth hormone secretion, connective tissue structure, muscle structure, vestibular dysfunction, melatonin secretion, and differences in platelet microstructure have been suggested as potential causes, the exact etiology of AIS remains unknown. Studies simplifying etiology to a single factor have been unsuccessful, indicating that the cause is multifactorial (2,3). While there are no widely accepted scientific theories for AIS etiology, studies focusing on pathogenesis have shown significant asymmetry in the pedicles of AIS individuals, which demonstrates clinical importance (4,5). In these studies, the concave side of the curve has been found to have reduced height and width periapically; the circumference of the pedicle on the convex side has been found to be sharper than that on the concave side around the apex (6). The identification of asymmetry between pedicles on the concave and convex sides in scoliosis patients minimizes the risk of screw placement complications and contributes greatly to understanding scoliosis etiology (6).

Scoliosis is assessed by the Cobb angle (a standard measurement method for determining the degree of curvature), which guides the decision between conservative approaches and surgical interventions in the management of AIS. The Cobb angle is obtained by drawing lines perpendicular to the upper and lower end vertebrae detected in the coronal plane of the X-ray (7,8). The Cobb angle is comprised of two basic components: the vertebral bodies and the intervertebral discs (7,9). The narrowing of the intervertebral disc space and wedging occurring in the vertebral bodies both influence the Cobb angle.

In this study, the researchers measured the heights of the concave and convex sides of vertebral bodies in patients with AIS and calculated the Cobb angle to investigate the impacts of the intervertebral disc and vertebral body heights on the overall Cobb angle.

MATERIAL AND METHODS

Ethical approval and study design

This study is retrospective and observational in nature. The researchers aimed to investigate the morphometric contribution of vertebral and discal wedging to the overall Cobb angle using radiographic and computed tomography (CT) data. The research was approved by the Bolu Abant Izzet Baysal University Clinical Researches Ethics Committee (Decision No: 2019/186). The medical records of patients diagnosed with AIS who received treatment at the Spine Clinic of Bolu Abant Izzet Baysal University Faculty of Medicine Training and Research Hospital between 2017 and 2020 were reviewed retrospectively.

Patient selection

Patients aged 13-18 years with a confirmed diagnosis of AIS whose available radiographs and CT images were suitable for accurate morphometric measurements (vertebral body and intervertebral disc heights on both the concave and convex sides of the spinal curve) were included in the study.

Patients who presented with congenital vertebral anomalies such as wedge or block vertebrae, lumbar disc herniation, or inflammatory back pain were excluded. Additional exclusion criteria included spinal conditions such as spondylolisthesis, rheumatologic or systemic disorders, and chronic pulmonary or cardiac diseases that might have affected spinal morphology. A total of 23 patients were found to be eligible for the study after these criteria were applied.

Radiographic and CT measurements

Demographic data (including age and sex) and radiological measurements (including Cobb angles, vertebral body heights, and intervertebral disc heights) were obtained for each patient. For quantitative evaluation, scoliosis radiographs in the anteroposterior plane and axial CT images were utilized.

Curvature assessment: In addition to the apical, neutral, and stable vertebrae, the upper and lower end vertebrae of the proximal thoracic, main thoracic, and lumbar curves were identified. The Cobb method on standing posteroanterior radiographs was utilized to calculate the magnitude of each curve.

Height measurements: On axial and sagittal CT images, the vertebral body and intervertebral disc heights on the concave and convex sides were measured. The narrowest and widest portions of the vertebral body and intervertebral disc were used to assess the degree of wedging. The respective contributions of these values to overall curvature were then identified by correlating the values with the Cobb angle values.

Statistical analysis

All statistical analyses were performed using IBM SPSS Statistics version 21.0 (IBM Corp., Armonk, NY, USA). Descriptive statistics were calculated for all variables. Continuous variables were expressed as mean, standard deviation, median, and range (minimum-maximum), while categorical variables were presented as frequencies and percentages. The Shapiro-Wilk test was applied to test the normality assumption for numerical variables. For paired comparisons between the concave and convex sides, the paired samples t-test was used in cases where the data were normally distributed, and the Wilcoxon signed-rank test was used where the data were not.

Pearson's correlation coefficient was used to assess the strength and direction of linear relationships between the total Cobb angle and its components, including the vertebral body Cobb angle and the disc Cobb angle. A p-value of less than 0.05 was considered statistically significant.

RESULTS

Of the 23 patients included in the study (aged 13-18 years), 82.6% were female and 17.4% were male; the mean age was 16.22 ± 1.59 years (Table 1).

Segment-level measurements of vertebral body heights and intervertebral disc heights between the upper and lower end vertebrae forming the Cobb angle are summarized in Table 2. Except for T4, the T4-T5 disc space, and T5, significant differences between concave and convex sides were observed for most vertebral levels (Table 2).

Descriptive statistics for the total Cobb angle, vertebral body (corpus), and disc components are presented in Table 3. The relationship between the corpus and disc components is illustrated in Figure 1. The associations of the total Cobb angle with the corpus and disc components are shown in Figures 2 and 3, respectively.

Correlation analysis demonstrated a moderate, statistically significant positive association between the total Cobb angle and the total vertebral body Cobb angle ($r = 0.698$, $p < 0.001$), and a strong, statistically significant positive correlation between the total Cobb angle and the total disc Cobb angle ($r = 0.894$, $p < 0.001$) (Table 4; see also Figures 2 and 3). In terms of variance explained, the corpus and disc components accounted for approximately 48.7% and 80.0% of the variability in the total angle, respectively (r^2 values derived from Table 4).

Table 1. Demographic characteristics of the participants (summary of participant characteristics including age and sex distribution (N = 23))

Variable	Category	Value
Sample size	N	23
Age	Mean ± SD	16.22 ± 1.59
	Range (min-max)	13 - 18
Sex	Female	19 (82.6%)
	Male	4 (17.4%)

Table 2. Descriptive statistics presenting mean, standard deviation, median [min - max] values are provided for the descriptive statistics

Level	n	Angle mean-SD	Angle median-min-max	Concave mean-SD	Concave median-min-max	Convex mean-SD	Convex median-min-max	p
T4	4	1.54 ± 1.83	1.73 [0.37-2.32]	1.78 ± 1.16	1.80 [1.60-1.92]	1.81 ± 1.19	1.83 [1.60-1.98]	0.180
T4-T5	4	2.39 ± 0.33	2.52 [1.90-2.60]	0.23 ± 0.06	0.23 [0.16-0.30]	0.25 ± 0.07	0.26 [0.20-0.35]	0.180
T5	9	2.04 ± 0.85	2.02 [0.93-3.88]	1.73 ± 0.13	0.72 [1.48-1.90]	1.75 ± 0.16	1.72 [1.48-2.02]	0.292
T5-T6	9	2.63 ± 0.88	2.45 [1.44-4.32]	0.23 ± 0.06	0.27 [0.10-0.29]	0.28 ± 0.07	0.28 [0.12-0.34]	0.002
T6	12	2.48 ± 0.77	2.58 [1.39-4.21]	1.75 ± 0.16	1.78 [1.38-2.00]	1.80 ± 0.16	1.81 [1.50-4.21]	0.035
T6-T7	12	2.85 ± 1.27	2.68 [0.79-5.74]	0.24 ± 0.08	0.25 [0.10-0.38]	0.31 ± 0.10	0.32 [0.11-0.49]	<0.001
T7	13	3.24 ± 1.08	3.45 [1.60-4.89]	1.77 ± 0.19	1.81 [1.38-2.06]	1.87 ± 0.17	0.89 [1.53-2.15]	<0.001
T7-T8	13	3.53 ± 2.98	2.98 [1.51-2.58]	0.26 ± 0.09	0.26 [0.11-0.42]	0.36 ± 0.14	0.37 [0.11-0.61]	0.003
T8	14	3.53 ± 1.06	3.41 [1.73-5.82]	1.82 ± 0.21	1.82 [1.43-2.12]	1.97 ± 0.18	2.03 [1.52-2.23]	<0.001
T8-T9	13	3.51 ± 2.02	3.21 [1.80-9.67]	0.27 ± 0.08	0.30 [0.13-0.38]	0.41 ± 0.14	0.42 [0.15-0.71]	0.001
T9	16	3.75 ± 1.87	3.09 [1.29-7.49]	1.89 ± 0.22	1.93 [1.46-2.22]	2.06 ± 0.21	2.13 [1.52-2.35]	0.001
T9-T10	16	3.31 ± 1.69	3.01 [1.78-8.90]	0.34 ± 0.11	0.36 [0.12-0.49]	0.46 ± 0.17	0.48 [0.21-0.87]	0.001
T10	17	3.44 ± 2.06	3.07 [1.02-0.39]	2.03 ± 0.19	2.05 [1.66-2.33]	2.19 ± 0.19	2.23 [1.79-2.48]	0.001
T10-T11	12	2.62 ± 0.60	2.56 [1.76-3.61]	0.38 ± 0.11	0.39 [0.20-0.55]	0.52 ± 0.18	0.49 [0.31-0.94]	0.002
T11	16	2.89 ± 0.99	2.87 [1.37-4.98]	2.18 ± 0.18	2.18 [1.72-2.50]	2.30 ± 0.17	2.33 [2.00-2.56]	0.001
T11-T12	15	2.97 ± 0.77	3.02 [1.64-4.12]	0.47 ± 0.12	0.50 [0.24-0.66]	0.65 ± 0.13	0.65 [0.43-0.86]	<0.001
T12	16	3.05 ± 1.16	2.73 [1.03-5.68]	2.29 ± 0.22	2.29 [1.78-2.70]	2.42 ± 0.18	2.41 [2.10-2.81]	<0.001
T12-L1	16	3.36 ± 1.21	3.41 [1.04-5.68]	0.50 ± 0.15	0.48 [0.20-0.94]	0.73 ± 0.18	0.75 [0.44-1.07]	<0.001
L1	16	3.24 ± 1.45	3.27 [1.19-6.09]	2.43 ± 0.23	2.45 [1.93-2.79]	2.56 ± 0.20	2.56 [2.22-2.89]	<0.001
L1-L2	15	4.12 ± 2.04	4.02 [1.90-9.73]	0.58 ± 0.15	0.55 [0.31-0.85]	0.87 ± 0.25	0.78 [0.56-1.49]	0.001
L2	15	3.08 ± 1.57	2.58 [0.71-6.16]	2.48 ± 0.22	2.47 [2.04-2.88]	2.61 ± 0.23	2.62 [2.27-3.00]	0.001
L2-L3	10	4.65 ± 2.62	3.48 [2.17-8.81]	0.64 ± 0.18	0.61 [0.35-0.93]	0.90 ± 0.21	0.91 [0.60-1.18]	0.001
L3	10	3.03 ± 1.23	2.67 [1.69-5.26]	2.55 ± 0.26	2.55 [2.23-2.93]	2.65 ± 0.26	2.69 [2.30-3.04]	0.005
L3-L4	8	3.58 ± 2.27	2.86 [1.66-8.96]	0.69 ± 0.22	0.70 [0.35-1.05]	0.86 ± 0.15	0.87 [0.57-1.10]	0.029
L4	8	2.07 ± 0.76	1.95 [1.00-3.26]	2.64 ± 0.26	0.64 [2.25-3.10]	2.76 ± 0.33	2.76 [2.24-3.30]	0.043

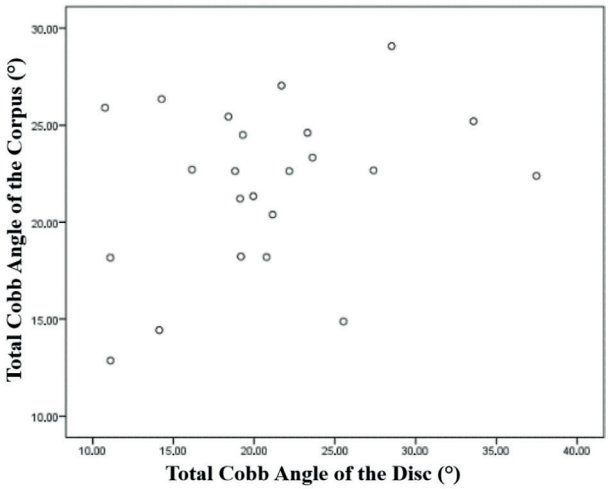

Figure 1. Scatter plot showing the relationship between the total vertebral body Cobb angle and the total disc Cobb angle.

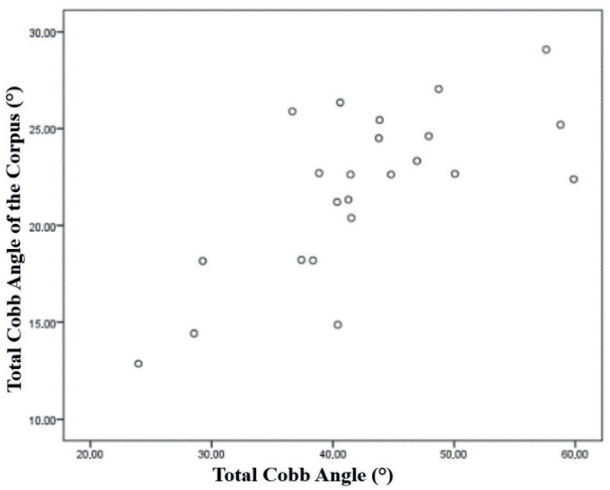

Figure 2. Scatter plot showing the relationship between the total vertebral body Cobb angle and the total Cobb angle.

Based on the decomposition of the total Cobb angle into its components, the mean proportional contributions were approximately 52% for the vertebral body component and 48% for the disc component; moreover, 65% of participants exhibited a larger corpus contribution to the total angle (visualized in Figure 4, with summary values in Table 3).

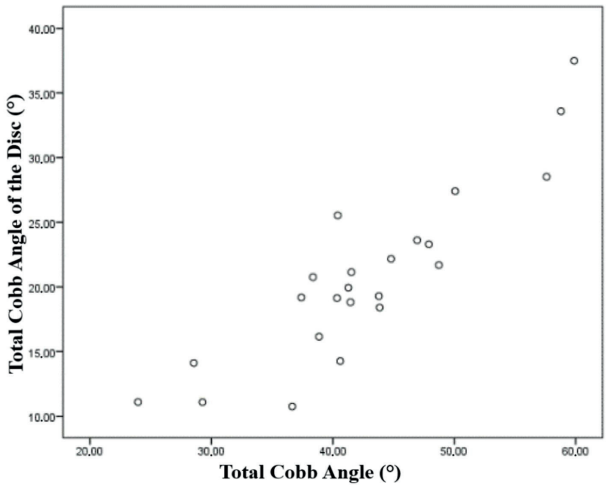

Figure 3. Scatter plot showing the relationship between the total disc Cobb angle and the total Cobb angle.

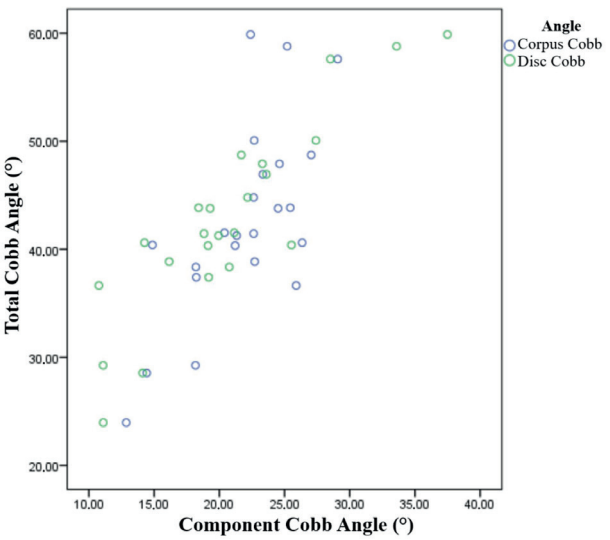

Figure 4. Scatter plot showing the distribution between vertebral body Cobb angle values and disc Cobb angle values.

Finally, the overall distributions and pairwise relationships among variables are depicted in Figures 1-4 and are consistent with the numerical results reported in Tables 1-4.

Table 3. Descriptive statistics of cobb angle values

Measurement	n	Mean	Standard Deviation	Median	Min - Max
Total Cobb Angle of the Corpus	23	21.92	4.19	22.63	12.86 - 29.08
Total Cobb Angle of the Disc	23	20.76	6.74	19.94	10.76 - 59.88
Cobb Angle	23	42.65	8.97	41.45	23.96 - 59.88

Table 4. Correlation between total cobb angle and vertebral/disc cobb angles

Comparison	r	p
Total Cobb Angle of the Corpus	0.698	<0.001
Total Cobb Angle of the Disc	0.894	<0.001

DISCUSSION

A major finding of this study was that vertebral body height on the concave side was consistently lower than on the convex side. Although the vertebral body component accounts for a slightly larger numerical share of the total Cobb angle, the intervertebral disc component demonstrates a stronger statistical correlation with the total angle. These findings suggest that disc wedging influences the pathogenesis and progression of spinal curvature in AIS more significantly (5-7,9). This concept is further corroborated by recent studies employing three-dimensional (3D) imaging and morphometric analyses, which argue that intervertebral disc deformation precedes vertebral structural remodeling, serving as an early biomechanical indicator of scoliosis progression (8,10,11). Studies conducted by Oba et al. (2025) and Labrom et al. (2020) demonstrated that higher discal asymmetry around the apical vertebra strongly correlates with a greater Cobb angle and more rapid curve progression. These findings underline the importance of disc wedging in the early stages of deformity formation (10,11).

Despite the critical importance of accurate morphometric characterization for surgical planning, morphometric studies on vertebral bodies and intervertebral discs in AIS remain relatively limited, with existing studies often involving small sample sizes.

To address this gap, Ramachandran et al. employed CT imaging to demonstrate significant vertebral and pedicle asymmetry in AIS patients, finding notable transverse plane deviations between the concave and convex sides (5). Qian et al.'s findings indicate that both vertebral height and width asymmetries contribute to rotational deformities and coronal curvature severity, aligning with more recent 3D CT-based investigations (8,12).

Huang et al. reported that disc wedging was the primary cause of curvature progression during the rapid growth phase, while vertebral body wedging became more prominent after skeletal maturation slowed (6). Shi et al. (2025) utilized automated SVD-based vertebral modeling to show that intervertebral disc compression dominates early deformity and subsequently transitions into bony remodeling as mechanical loading asymmetry persists (13). Our findings are consistent with these studies and suggest a dynamic anatomical shift in deformity contributors over time.

Shen et al. demonstrated that vertebral wedging tends to increase toward the apex of the scoliotic curve, particularly in the coronal plane, while sagittal wedging remains minimal (7). Recent imaging-based studies have corroborated this apex-centric distribution, indicating that maximal structural asymmetry occurs at the apical region and diminishes progressively toward the end vertebrae (14). The observation of decreased vertebral and disc height differences as the distance from the apex increases supports this progressive wedging gradient.

In addition, Qian et al. demonstrated anterior-posterior length disparities in the thoracic region of AIS patients, primarily attributed to soft tissue and discal alterations rather than bone morphology (8). Similarly, Wang et al.

(2025) observed that asymmetric disc loading induces significant shear stress at the endplates, predisposing vertebral wedging through altered growth plate pressure distribution (15).

In a study by Okuwaki et al., regional wedging patterns were differentiated, showing that vertebral body wedging is more prominent in thoracic curves, whereas disc wedging is more pronounced in lumbar deformities (9). These region-specific variations were confirmed in recent finite element modeling studies by Zhang et al. (2025), which demonstrated that lumbar disc wedging has a more substantial impact on spinal flexibility and curve reversibility compared to thoracic vertebral wedging (16).

Beyond osseous and discal morphology, neurodevelopmental and myofascial factors have gained attention as modulators in AIS progression. It is hypothesized that neuroanatomical asymmetries and proprioceptive dysfunctions may alter postural control and loading symmetry, contributing to progressive curvature (17,18). Zhang et al. (2025) further demonstrated via shear-wave elastography that asymmetry in paraspinal muscle stiffness correlates strongly with vertebral body wedging, emphasizing the interaction between muscle and bone in AIS biomechanics (19).

Our findings also parallel the MRI-based study by Labrom et al., which revealed that vertebral body wedging significantly contributes to coronal deformity during growth spurts (20). Similarly, Zhang et al. (2025) confirmed that "relative anterior spinal overgrowth" is a key structural phenomenon underlying curve progression, especially in moderate AIS (14). Collectively, these findings reinforce the idea that discal deformation likely initiates curvature, while vertebral wedging sustains and stabilizes it as growth progresses.

Standardized nomenclature for vertebral and disc geometry has been advocated to improve scoliosis research (21). Our CT-based quantification approach aligns with these recommendations and supports the transition toward multi-parametric, 3D diagnostic evaluation.

In summary, this study underscores that both vertebral and discal structures contribute significantly to the Cobb angle in AIS. While vertebral wedging quantifies cumulative deformity, disc wedging may better reflect active curve progression. Integrating 3D morphometric, biomechanical, and neuromuscular parameters can enhance diagnostic precision and guide individualized therapeutic strategies for AIS (10-22).

Limitations

The study was limited by: (i) the relatively small sample size (n = 23), which may affect statistical power and limit generalizability; (ii) its single-center design, which introduces potential selection bias; (iii) possible measurement errors or interobserver variability, despite the use of high-resolution CT; and (iv) its retrospective nature, which limits control over confounding variables such as growth status or prior treatments. Future multicenter, prospective studies with larger cohorts are required to validate these findings.

CONCLUSION

This study established that both vertebral body and intervertebral disc wedging contribute significantly to the Cobb angle in AIS. While vertebral body wedging shows a slightly higher numerical contribution, disc wedging exhibits a stronger correlation with overall curvature, indicating a predominant role in curve progression. The results suggest that the relative decrease in vertebral and disc heights on the concave side, particularly near the apex, is critical to the three-dimensional deformity in scoliosis.

Improved understanding of the morphometric dynamics of spinal curvature can enhance diagnostic precision and help identify progressive curves earlier. Quantifying the separate contributions of disc and vertebral wedging and incorporating detailed imaging metrics into clinical decision-making may: (i) aid in developing targeted conservative approaches; (ii) guide surgical strategies; and (iii) improve individualized treatment planning and long-term outcomes for patients with idiopathic scoliosis.

The researchers also suggest that future studies with larger sample sizes and longitudinal designs would both validate these morphometric patterns and help better understand their role in monitoring prognosis and therapeutic response thereafter.

Ethical approval

This study has been approved by the Bolu Abant Izzet Baysal University Clinical Researches Ethics Committee Approval (approval date 18/12/2019, number 2019/186).

Author contribution

Concept: MK, Cİ; Design: MK, CA; Data Collection or Processing: MMB, EA; Analysis or Interpretation: MÇ, MTT; Literature Search: MK; Writing: MK, CA. All authors reviewed the results and approved the final version of the article.

Source of funding

The authors declare the study received no funding.

Conflict of interest

The authors declare that there is no conflict of interest.

REFERENCES

1. Abasi U, Allen A, Candelario-Velazquez C, Ranade S, Cancel D. Management of Hip and Spine in Neuromuscular Disorders. Phys Med Rehabil Clin N Am. 2025; 36(3): 429-45. **[Crossref]**
2. Splittgerber R. Snell's Clinical Neuroanatomy. Lippincott Williams & Wilkins; 2024.
3. Erguven SP. Development of Spinal Cord and Malformations. In: Yucel N, Hekimoglu G, editors. Health & Science 2024: Basic Medical Sciences - Central Nervous System. Istanbul: Efe Academy; 2024: 173-94.
4. Alshryda S, Jones S, Banaszkiewicz PA, editors. Postgraduate Paediatric Orthopaedics: The Candidate's Guide to the FRCS (Tr&Orth) Examination. Cambridge: Cambridge University Press; 2024. **[Crossref]**
5. Ramachandran K, Naik AS, Thippeswamy PB, Shetty AP, Kanna RM, Rajasekaran S. Curve magnitude and vertebral rotation influence the MRI predictability of pedicle dimensions in adolescent idiopathic scoliosis: an analysis of 1,860 pedicles. Spine Deform. 2025; 13(6): 1819-29. **[Crossref]**
6. Huang X, Luo M, Liu L, et al. The Comparison of Convolutional Neural Networks and the Manual Measurement of Cobb Angle in Adolescent Idiopathic Scoliosis. Global Spine J. 2024; 14(1): 159-68. **[Crossref]**
7. Shen Y, Qin F, Pan Y, et al. Correlation between coronal wedge deformity and sagittal spinal curvature in adolescent idiopathic scoliosis: a retrospective analysis. Sci Rep. 2024; 14(1): 29038. **[Crossref]**
8. Qian L, Jiang Y, Zhang T, Sun K, Xu X, Yu J. 3D CT analysis of vertebral morphology in adolescent scoliosis and its severity correlation. Journal of Radiation Research and Applied Sciences. 2025; 18(4): 101948. **[Crossref]**
9. Okuwaki S, Kotani T, Sunami T, et al. Associated factors and effects of coronal vertebral wedging angle in thoracic adolescent idiopathic scoliosis. J Orthop Sci. 2024; 29(3): 704-10. **[Crossref]**
10. Oba H, Kelly MP, Fletcher N, et al. Three-Dimensional Analysis of Disc and Vertebral Height and Their Role in Kyphosis Creation in Adolescent Idiopathic Scoliosis. Spine (Phila Pa 1976). 2025; 50(23): 1617-23. **[Crossref]**
11. Labrom FR, Izatt MT, Contractor P, et al. Sequential MRI reveals vertebral body wedging significantly contributes to coronal plane deformity progression in adolescent idiopathic scoliosis during growth. Spine Deform. 2020; 8(5): 901-10. **[Crossref]**
12. Li L. Development of 3D spatial measurement method based on computed tomography images of adolescent idiopathic scoliosis [dissertation]. Hong Kong: The Hong Kong Polytechnic University; 2025.
13. Shi C, Meng N, Zhuang Y, et al. Accurate Cobb Angle Estimation via SVD-Based Curve Detection and Vertebral Wedging Quantification. IEEE J Biomed Health Inform. 2025; 29(12): 8607-14. **[Crossref]**
14. Zhang H, Ye X, Wu H, et al. Relative anterior spinal overgrowth in mild and moderate adolescent idiopathic scoliosis: a retrospective study. Sci Rep. 2025; 15(1): 2651. **[Crossref]**
15. Wang H, Ma Z, Wu Z, et al. Biomechanical analysis of spinal range of motion and intervertebral disc loadings in normal and adolescent idiopathic scoliosis models. Front Bioeng Biotechnol. 2025; 13: 1473776. **[Crossref]**
16. Zhang T, Gu X, Li H, Wu C, Zhao N, Peng X. Statistical Shape Modeling and Prediction of Lumbar Spine Morphology in Patients With Adolescent Idiopathic Scoliosis. J Biomech Eng. 2025; 147(5): 051002. **[Crossref]**
17. Singh V. Textbook of Clinical Neuroanatomy - E-Book. Elsevier Health Sciences; 2024.
18. Grivas TB, Vasiliadis E, Soultanis K, et al. Idiopathic Scoliosis Progression: Presenting Rib and Segmental Rib Index as Predictors-A Literature Review. Med Sci (Basel). 2025; 13(2): 62. **[Crossref]**
19. Zhang H, Ye X, Pan Y, et al. Evaluation of paraspinal muscles in adolescent idiopathic scoliosis: a study based on shear wave elastography. Spine Deform. 2025; 13(5): 1391-7. **[Crossref]**

20. Labrom FR, Izatt MT, Askin GN, Labrom RD, Claus AP, Little JP. Segmental deformity markers offer novel indicators of deformity progression risk in deformity-matched adolescent idiopathic scoliosis patients. Spine Deform. 2024; 12(6): 1647-55. **[Crossref]**

21. Wei W, Cheng L, Dong Y, et al. 2D and 3D Classification Systems for Adolescent Idiopathic Scoliosis: Clinical Implications and Technological Advances. Orthop Surg. 2025; 17(4): 999-1020. **[Crossref]**

22. Gay M, Cobetto N, Caouette C, et al. Patient-specific biomechanical modeling of intraoperative scoliosis correction on the 2-year outcomes for thoracolumbar/lumbar vertebral body tethering. Spine Deform. 2026; 14(1): 31-8. **[Crossref]**